Integral and Nonintegral Folding in Lamellar Crystals of Molecular Complexes of Poly(ethylene oxide)

L. Paternostre, P. Damman,† and M. Dosière*

Laboratoire de Physico-Chimie des Polymères, Université de Mons-Hainaut, 20, place du Parc, B-7000 Mons, Belgium

C. Bourgaux

Lure, Centre Universitaire de Paris-Sud, Bat. 209 D, F-91403 Orsay Cedex, France

Received May 10, 1995; Revised Manuscript Received December 1, 1995[⊗]

ABSTRACT: The morphology of poly(ethylene oxide) (PEO) complexes crystallized from the melt is investigated by small angle X-ray scattering and differential scanning calorimetry. The formation of integral folded chain crystals with either extended chains (EC) or *x*-folded chains is observed for the PEO−resorcinol complex. As for pure PEO oligomers, the fraction of EC crystals increases with the crystallization temperature to give finally only EC crystals but in a larger range of crystallization temperatures. On the other hand, the PEO−*p*-nitrophenol complex crystallizes over all the studied temperature range as stable nonintegral folded chain crystals. These two different lamellar morphologies are related to the crystal structure of these complexes and their mode of growth.

Introduction

The crystallization and morphology of poly(ethylene oxide) (PEO) oligomers have been extensively investigated.[1−6] The PEO macromolecules are found to crystallize either with an integral number of folds ($n \geq 1$) or with an extended chain conformation ($n = 0$).[1,4] Kovacs et al.[4] have related the breaks observed in the growth rate curves of spherulites and single crystals of low molecular weight PEO to a stepwise change in the lamellar thickness. Indeed, transition temperatures were assigned to these breaks. In each range of crystallization temperatures, limited by two consequent breaks, the thickness of the lamellar crystals correspond either to extended chain crystals or to *x*-folded chain crystals. Such a behavior was observed for PEO oligomers with molecular weights ranging between 2000 and 20 000. Raman longitudinal acoustic mode (LAM),[7] calorimetry,[8,9] and SAXS[1−3] data indicate that the chain ends formed by OH groups are localized at the surface of the lamellae, the PEO chain axes being perpendicular to these surfaces. A noninteger form (NIFC) of lamellar crystals of oligomers of PEO has been observed by LAM[10] and SAXS.[11,12] These NIFC crystals are associated with the early stages of crystallization, transforming with time into integral folded chain (*x*IFC) crystals.[11,12] A mechanism involving a thickening or a thinning process was assumed to account for the transformation of NIFC crystals into these *x*IFC crystals ($x = 0$ or 1). Recently, Krimm et al.[13] showed by time-resolved LAM that the PEO chains are inclined with respect to the lamellar surfaces in NIFC crystals. On conversion to extended or one-folded chain crystals, the chain axes become perpendicular to the lamellar surface.

PEO forms various crystalline molecular complexes with inorganic[14−17] and organic[18−24] compounds. More particularly, molecular complexes have been reported between PEO and hydroxybenzenes such as resorcinol,[19,20] 2-methylresorcinol,[21] 5-methylresorcinol,[21] hydroquinone,[21−23] and *p*-nitrophenol.[24,25]

Table 1. Average Molecular Weights and Polydispersity of PEO Oligomers

sample	$\langle M_n \rangle$	$\langle M_w \rangle$	polydispersity
6K	5425	5940	1.09
10K	11 456	12 220	1.07
35K	29 239	33 100	1.13

The phase diagram of PEO−resorcinol (PEO−RES) presents a bell-shaped region centered around a 2:1 molar stoechiometry (i.e., two PEO monomer units for one resorcinol molecule) which separates two eutectics. This molecular complex can crystallize in two allotropic forms,[20] called α- and *β*-forms. The *β*-form is metastable and transforms into the stable α-form.[26] The melting temperatures for the α- and *β*-forms of the PEO−RES molecular complex (PEO molecular weight equal to 6000) are 93 and 73 °C, respectively.[20]

The phase diagram of the PEO−*p*-nitrophenol (PEO−PNP) system exhibits the characteristics of an eutectic−peritectic system.[25] The molecular complex has the same molar fraction as the second eutectic, i.e., $X_{PEO} = 0.6$; its melting temperature is 95 °C (the molecular weight of PEO used being equal to 6000).

The aim of this paper is to study the lamellar structure of crystals of these two molecular complexes in comparison with that of pure PEO. An attempt to correlate the different lamellar morphologies of crystals of PEO−RES and PEO−PNP molecular complexes taking into account their crystal structure and their mode of crystal growth is presented.

Experimental Section

Materials. PEO samples having low molecular weights approximately equal to 6000, 10 000, and 35 000 and called PEO6K, PEO10K, and PEO35K, respectively, were kindly provided by Hoechst. The molecular weight distribution of the PEO oligomers was determined by size exclusion chromatography at 25 °C in tetrahydrofuran. The characteristics of these PEO oligomers are given in Table 1. The preparation of the molecular complexes was already described elsewhere[20,24] and is therefore briefly recalled. The PEO molecular complex inserted between two glass sides was melted at 110 °C and afterwards was quickly transferred in a hot stage (Mettler

* To whom correspondence should be addressed.
† Research Associate of the Belgian National Fund for Scientific Research.
⊗ Abstract published in *Advance ACS Abstracts,* February 1, 1996.

0024-9297/96/2229-2046$12.00/0

FT82HT and FP90) and kept at the chosen crystallization temperature for 10 h at least. Polarized optical microscopy was used to check the completion of the crystallization process at high crystallization temperatures.

Characterization. A Perkin Elmer differential scanning calorimeter (DSC 4 model) fitted with a TADS computing station and a low-temperature cooling accessory was used to record the melting curves. The scanning rates were 2, 10, and 20 K/min. Azobenzol, benzoic acid, and indium were used for the calibration of the temperature axis. The melting temperatures are given with a precision of ±0.5 °C.

Wide (WAXS) and small (SAXS) angle measurements were carried out with a Rigaku 6kW rotating anode generator delivering Cu Kα X-rays. A Kiessig camera with a pinhole collimation modified in order to record simultaneously the WAXS and SAXS patterns was used. SAXS intensity measurements were conducted at the D24 beam line of the LURE-DCI synchrotron radiation facility (Lure, Centre Universitaire de Paris-Sud, Orsay, France). The monochromator was a single bent Ge crystal with a (111) plane. The wavelength of the incident X-ray beam was 0.149 nm. The distance between the sample and the detecting plane was 3 m. The SAXS intensity curves were recorded with a linear position detector or image plates (Molecular Dynamic 445 type reader). The SAXS intensity raw data were firstly normalized with respect to the intensity of the incident beam. Afterwards, after background substraction, the Lorentz corrections were applied as usual. The electron density correlation function, $\gamma(d)$, was calculated from the corrected SAXS intensity data using the relation

$$\gamma(d) = \frac{\int_0^\infty I(s)s^2 \cos(2\pi sd)\, ds}{\int_0^\infty I(s)s^2\, ds}$$

where $s = 2 \sin \theta/\lambda$ (2θ and λ being the diffraction angle and the wavelength of the X-ray beam). The $\gamma(d)$ functions were normalized to obtain $\gamma(0) = 1$. The relative volume degree of crystallinity (v_c) can be easily calculated from the correlation function.

Results and Discussion

Crystal and Molecular Structure. The crystal structure of the α-form of the PEO−RES molecular complex was obtained from the analysis of two fiber patterns: a stretched sample with the *c*-crystallographic parameter as fiber axis and a spherulitic sample with the *a**-reciprocal parameter along the radius of the spherulite.[20] Spherulites of PEO−RES molecular complex having a diameter of 10 mm and a thickness of 20−30 μm can be obtained by a good control of the crystallization parameters. As the diameter of the pinhole collimation system used to record the WAXS pattern was 0.3 mm, the experimental conditions were quite filled to obtain a fiber pattern where the radii of the spherulite were parallel in the X-ray irradiated part. The unit cell obtained from this analysis of two fiber patterns is orthorhombic and contains eight monomeric units and four resorcinol molecules. The crystallographic parameters are $a = 1.050$ nm, $b = 1.018$ nm, and c (chain axis) $= 0.978$ nm. The spatial group, determined from the systematic extinctions found in the two fiber X-ray patterns, is $Pna2_1$. From WAXS and polarized Fourier transform infrared spectroscopy data, a 4/1 helical conformation was proposed for the PEO chains in the PEO−RES molecular complex. This conformation is very similar to the 7/2 helix of pure PEO, although the length of the pitch period is 0.978 nm (the length of a PEO monomeric unit is therefore 0.2445 nm in PEO−RES molecular complex) (Figure 1). The analysis of the WAXS pattern indicates that, in all

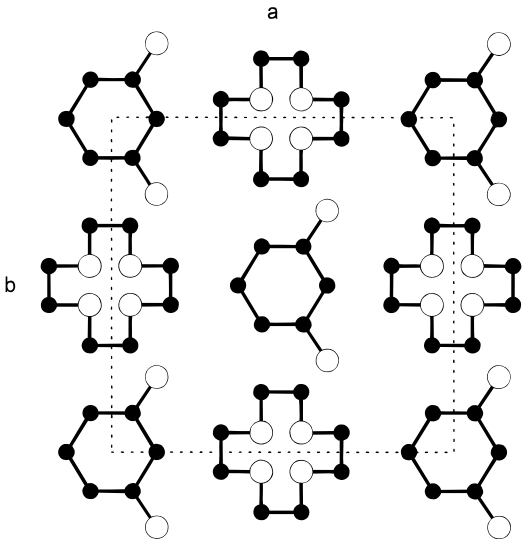

Figure 1. Crystal structure of the poly(ethylene oxide)−resorcinol molecular complex.

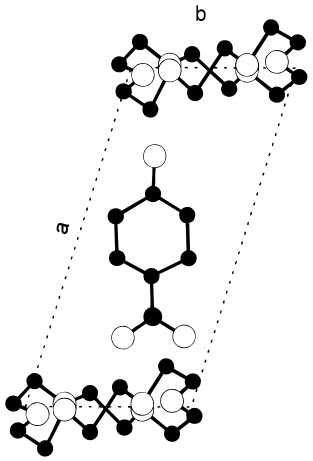

Figure 2. Crystal structure of the poly(ethylene oxide)−*p*-nitrophenol molecular complex.

the investigated crystallization temperature range, the (100) crystallographic plane is perpendicular to the spherulite radius, i.e., that the *a**-reciprocal axis is along the radius of the spherulite.

The PEO−PNP molecular complex has a triclinic unit cell with the following crystallographic parameters: $a = 1.172$ nm, $b = 0.555$ nm, $c = 1.557$ nm, $\alpha = 90.7°$, $\beta = 87.1°$, and $\gamma = 104.0°$ with a P_{-1} space group. The unit cell contains six PEO monomers and four *p*-nitrophenol molecules stacked along the *c*-crystallographic axis[24,25] (Figure 2). Contrary to the PEO−RES complex, the PEO chains adopt an unusual glide type conformation ($t_2gt_2gt_3$) stabilized by hydrogen bonds between host and guest molecules. This conformation is quite different from the 7/2 helical conformation of pure PEO. From the joint study of the morphology and growth of PEO−PNP spherulites, we have shown that the curve giving the thermal dependence of the growth rate of PEO6K−PNP spherulites exhibits two breaks related to a change of the growth face.[24] For crystallization temperatures ranging from room temperature to 58 °C and above 65 °C, the growth face is parallel to the (100) crystallographic facet. Between 58 and 65 °C, the crystallization of a (010) leading facet is observed. From the structure of the molecular complex (Figure 2), the growth of PEO−PNP spherulites occurs following an alternate deposit of PNP molecules and PEO layers

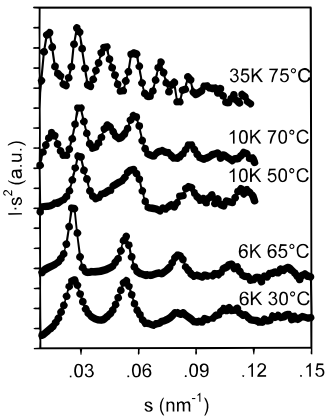

Figure 3. Selected Lorentz-corrected SAXS intensity curves of PEO−RES spherulitic samples made with PEO having molecular weights around 6000, 10 000, and 35 000, noted as PEO6K, PEO10K, and PEO35K.

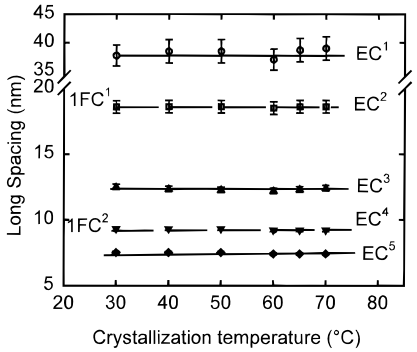

Figure 4. Long spacing of PEO6K−RES versus the crystallization temperature. EC^n and 1IFC^n refer to the nth order of the EC and 1IFC crystals, respectively.

at crystallization temperatures below 58 °C and above 65 °C.

SAXS Measurements and Differential Scanning Calorimetry. Assuming that the samples of molecular complexes used for SAXS intensity measurements consist of isotropically distributed stacks of parallel lamellae, an estimate of the long spacing, L, corresponding, in the two-phase model, to the sum of the thicknesses of a crystalline core, L_c, and an amorphous region, L_a, can be derived by applying the Bragg law to the Lorentz-corrected SAXS intensity data. On the other hand, the electron density correlation function provides more detailed informations about the supermolecular structure of semicrystalline polymers[27,28] such as the most probable long period, the average lamellar thickness, and the volume degree of crystallinity.

PEO−RES Molecular Complexes. Some typical SAXS intensity curves of PEO−RES molecular complexes with PEO of different molecular weights are shown in Figure 3. The SAXS intensity curves of PEO6K−RES molecular complex crystallized from the melt between 30 and 75 °C contain five (even six) well-resolved diffraction peaks. The Bragg spacings are equal to 38.2, 18.6, 12.3, 9.2, and 7.4 nm and appear to be insensitive to the crystallization temperature (Figure 4). These peaks are the first five orders of a long spacing equal to 38.2 nm corresponding to a full extended PEO chain. Such a large number of orders of the long spacing points the regularity of the thickness and the stacking of lamellar crystals in the PEO−RES spherulites. As proposed by Arlie et al.,[1] an average molecular weight, $\langle M_n^* \rangle$, can be correlated to the observed long spacings following the relation

$$\langle M_n^* \rangle = L(M_{ru}/L_{ru}) = L180.176 \text{ nm}^{-1}$$

where L, M_{ru}, and L_{ru} are the lamellar thickness (in nm), the molecular weight of the repeat unit (176.212 Da), and its length (0.9780 nm), respectively.

Table 2. Lamellar Thickness and Related Number-Average Molecular Weights of PEO−RES Molecular Complexes[a]

sample	L (nm)	$\langle M_n^* \rangle$	$\langle M_n \rangle$, GPC
6K EC	38.2	6882	5425
6K 1IFC	18.6	6702	5425
10K EC	65.9	11 874	11 456
10K 1IFC	33.9	12 216	11 456
35K 2IFC	73	39 460	29 239

[a] The $\langle M_n^* \rangle$ number-average molecular weight is obtained by multiplying the value of the lamellar thickness (in nm) by 180.176 nm^{-1}, which corresponds to the weight (in Da) of a PEO stem of 1 nm.

The comparison between $\langle M_n^* \rangle$ and GPC values (Table 2) is based on the following assumptions. (i) The length of the amorphous layer is negligible with respect to the lamellar thickness (ν_c is larger than 0.9). (ii) The chain axes are normal to the plane of the lamellae. This last assumption is in agreement with the study reported by Krimm et al.[13] In fact, the crystallization of lamellae with inclined chain axis was only observed for NIFC crystals, IFC crystals having their chain axes always normal to the basal plane of the lamellae. For PEO6K−RES, the calculated value of $\langle M_n^* \rangle$ is equal to 6847 and higher than the value obtained by GPC. The discrepancy between the average number molecular weights, $\langle M_n \rangle$, and $\langle M_n^* \rangle$ obtained by size exclusion chromatography and SAXS measurements, respectively, is very likely due to the polydispersity of the PEO samples.[3] The GPC trace of PEO6K exhibits an important low molecular tail which contributes to lower the number-average molecular weight. On the other hand, the thickness of the lamellar crystals is mainly determined by the length of the longest PEO chains.

The direct analysis of the Lorentz-corrected SAXS intensity curves is ambiguous because of the possible overlapping of the different peaks corresponding either to the nth order of the long spacing or to different lamellar thicknesses. In the case of a mixture of EC and 1IFC crystals, for example, the second peak (18.6 nm) can be attributed either to the second order of EC crystals (EC^2) or to the first order of 1IFC crystals (1IFC^1). In order to solve this problem, the correlation functions have been calculated from the corrected SAXS intensity data of PEO6K−RES[27,28] (Figure 5). For crystallization temperatures between 30 and 60 °C, the correlation functions exhibit two peaks at 19.5 and 37.5 nm, which can be unambiguously related to 1IFC and EC lamellar thicknesses. The magnitude of the 1IFC peak (19.5 nm) is low and continuously decreases with increasing crystallization temperature to finally disappear for samples crystallized at temperatures higher than 65 °C. The analysis of the correlation function curves shows that PEO6K−RES samples crystallized between room temperature and 60 °C are mixtures of extended chain (EC) crystals and one-integral folded chain (1IFC) crystals, the fraction of EC crystals increasing with the crystallization temperature. By comparison, the pure PEO6K oligomers crystallize with EC only for crystallization temperatures very near the melting temperature. The volume degree of crystallin-

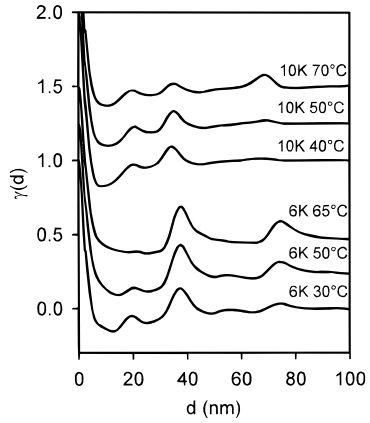

Figure 5. Correlation functions of PEO6K−RES and PEO10K−RES molecular complexes crystallized from the melt at 30, 50, and 65 °C and at 40, 50, and 70 °C, respectively.

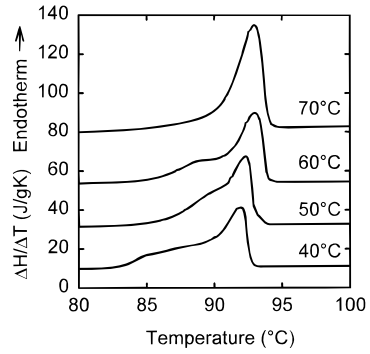

Figure 6. Melting curves of PEO6K−RES samples crystallized from the melt at different temperatures (heating rate: 10 °C/min).

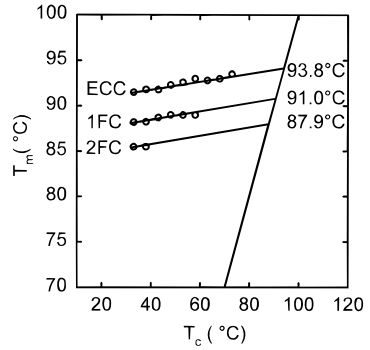

Figure 7. Melting temperature of PEO6K−RES samples isothermally crystallized versus the crystallization temperature. The equilibrium melting temperatures, T_m^0, of EC, 1IFC, and 2IFC crystals are also given (heating rate: 10 °C/min).

ity can be computed from the correlation function and is found to range between 0.85 and 0.95 for the different PEO6K−RES samples. The coexistence of *x*IFC crystals and EC crystals in samples crystallized between 30 and 60 °C is also supported by DSC analysis as shown hereafter. The melting curves of PEO6K−RES samples crystallized at different crystallization temperatures contain several melting peaks (Figure 6). The observed melting temperatures, T_m, are given against the crystallization temperature in Figure 7. At high crystallization temperatures, i.e., for $T_C > 60$ °C, a single endothermic peak is observed. This peak is characterized by a high melting temperature (93.0 ± 0.5 °C) and can be attributed unambiguously to the melting of EC crystals. At intermediate crystallization temperatures (40 °C < $T_c \leq 60$ °C), the melting curves show a prominent peak and a shoulder with its maximum centered at 89.0 ± 0.5 °C. Referring to the SAXS data already discussed above, this shoulder results from the melting of one-folded chain lamellar crystals. The relative area of the main peak in the DSC curve corresponding to EC crystals increases with increasing crystallization temperatures, as already deduced from the analysis of the SAXS correlation functions. At low crystallization temperatures ($T_C < 40$ °C), the melting behavior becomes more complex. The low-temperature shoulder in the DSC curve broadens and can be resolved into two peaks, suggesting the coexistence of lamellar crystals with three different thicknesses, i.e., EC, 1IFC, and 2IFC crystals. The equilibrium melting temperatures of these different lamellar crystals have been estimated to be 93.8, 91.0, and 87.9 °C for EC, 1IFC, and 2IFC, respectively. Despite the increase of the melting temperature of PEO molecular complexes with respect to the melting temperature of pure PEO oligomers, the difference between the melting temperatures of EC and 1IFC crystals is around 3 °C, a value similar to that reported for pure PEO6K oligomers[8,9](the melting temperatures of EC and 1IFC PEO crystals are 63.3 and 60.7 °C, respectively). The slight increase of the melting temperature of EC, 1IFC, and 2IFC lamellar crystals with respect to the crystallization temperature results from an improvement of the perfection of the *x*IFC crystals as already reported for PEO lamellar crystals.[8,9] The occurrence of several melting peaks in the DSC trace of PEO6K−RES molecular complex samples crystallized below 65 °C (Figure 6) confirms the conclusions already deduced from the analysis of the SAXS intensity data: the coexistence of *x*IFC crystals with EC crystals. The melting curves of a PEO6K−RES sample crystallized at 60 °C have been recorded at different heating rates ranging from 2 to 20 °C/min (Figure 8). At the highest heating rate (20 °C/min), it can be assumed that the area of the endotherms is a good approximation of the true proportion of EC and 1IFC crystals because the reorganization processes of 1IFC crystals into EC crystals during the heating in the calorimeter can be neglected. At the low heating rate (2 °C/min), the disappearence of the low-temperature endotherm, assigned to the melting of 1IFC crystals, and the increase in magnitude of the area of the high-temperature endotherm indicate that the unfolding of 1IFC crystals into EC crystals occurs for the PEO6K−RES molecular complex. It must also be mentioned that the relative proportion of EC and *x*IFC crystals depends on the crystallization time as shown by time-resolved SAXS intensity measurements.[29]

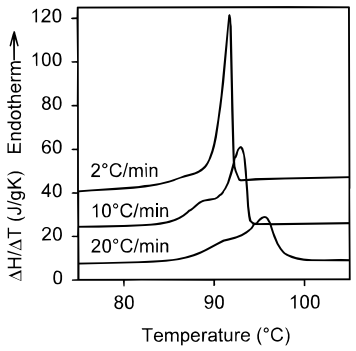

Figure 8. Melting curves of a PEO6K−RES sample crystallized at 60 °C recorded at different heating rates indicated in the graph.

Similar experiments were performed on PEO10K−RES and PEO35K−RES molecular complexes. Typical Lorentz-corrected SAXS intensity curves of PEO10K−

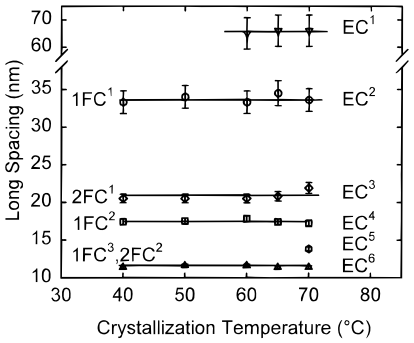

Figure 9. Long spacing of PEO10K−RES versus the crystallization temperature. EC^n and $1IFC^n$ refer to the *n*th order of the EC and 1IFC crystals, respectively.

RES crystallized at 50 and 70 °C are given in Figure 3. The spacings corresponding to the different maxima observed in the Lorentz-corrected SAXS intensity curves of PEO10K−RES crystallized between 40 and 70 °C are equal to 65.9, 33.9, 21.4, 17.4, 13.8, and 11.5 nm (Figure 9). The spacing of 65.9 nm corresponds to the long spacing of EC crystals. The spacing of 21.4 nm can be attributed either to the third order (EC^3) of extended chain crystals or to the first order of two-folded chain ($2IFC^1$) crystals. The spacing of 13.8 nm, corresponding to the fifth order of the lamellar thickness of EC crystals (EC^5), is only observed in the SAXS curve of the sample crystallized at 70 °C. Therefore, if extended chain crystals can be obtained at low crystallization temperatures, it is only by crystallization at higher temperatures, such as 70 °C, that regular stacks of extended chain lamellar crystals can be obtained. A more quantitative analysis of the SAXS intensity data of PEO10K−RES samples crystallized at 40, 50, 65, and 70 °C can be made from the calculated correlation functions (Figure 5). Two maxima are well observed in the correlation function of samples crystallized at 40 and 50 °C. They are characteristic of 1IFC and 2IFC crystals. A third maximum with a spacing of 68.5 nm is well observed for crystallization temperatures equal to and higher than 65 °C. PEO10K−RES molecular complex samples crystallized at temperatures equal to and lower than 50 °C mainly contain 1FC crystals. The $\langle M_n^* \rangle$ number-average molecular weight estimated from the long spacing of EC crystals (66 ± 1.5 nm) is found to be equal to 11 892, a slightly higher value than the value of 11 450 obtained by GPC measurements (Table 2). The reason for such a discrepancy has been already presented in the comments of the SAXS data of PEO6K−RES.

Only partial results on the crystallization of the PEO35K−RES molecular complex are now available taking into account the required measurement of ultralong spacing such as 150−250 nm to check for the occurrence of EC or 1IFC crystals from the SAXS intensity curves. Nevertheless, the corrected Lorentz SAXS intensity curve of a PEO35K−RES sample crystallized at 75 °C contains several diffraction peaks (Figure 3). The values of these spacings are 73, 36, 24, and 18 nm, indicating the occurrence of 2IFC crystals. A more detailed investigation of the crystallization of PEO35K−RES and PEO20K−RES is in progress.

PEO−PNP Molecular Complexes. Two broad peaks are observed in the SAXS intensity curves of PEO6K−PNP and PEO35K−PNP crystallized from the melt between room temperature and 70 °C (Figure 10). These two spacings can be related to the first and second orders of the same lamellar thickness. In opposite to

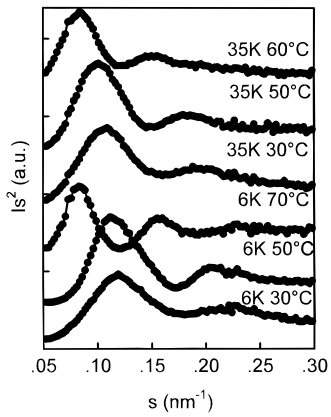

Figure 10. Selected Lorentz-corrected SAXS intensity curves of PEO6K−PNP and PEO35K−PNP molecular complexes crystallized from the melt at various temperatures.

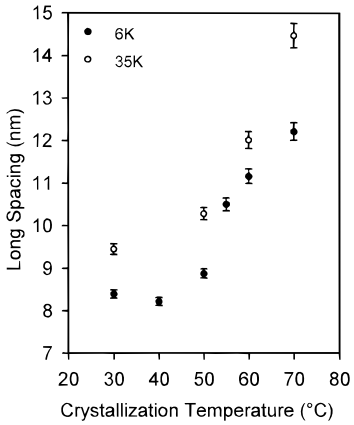

Figure 11. Long spacing of PEO6K−PNP and PEO35K−PNP versus the crystallization temperature.

the observations about the PEO−RES molecular complex, the long spacing continuously increases with the crystallization temperature from 8.4 to 12.2 nm and from 9.5 to 14.5 nm for complexes made of PEO having molecular weights of 6000 and 35 000, respectively (Figure 11). Surprisingly, neither EC nor *x*IFC crystals are present in the PEO−PNP samples. By considering the length of an extended chain of PEO6K or PEO35K (Table 1), these long spacing data imply that the PEO−PNP spherulitic samples are made of stable nonintegral folded chain crystals. The width of the SAXS peaks points to a broad distribution of the lamellar thicknesses of these NIFC crystals. The correlation functions were also calculated and show only one lamellar thickness. However, we should note that the volume crystallinities in PEO−PNP NIFC lamellar stacks computed from the correlation functions are also very high and range between 0.75 and 0.85, depending upon the crystallization temperature. The formation of NIFC crystals is thus found to only slightly affect the crystallinity in the lamellar stacks.

The melting curves of PEO6K−PNP samples crystallized at various temperatures ranging from 40 to 70 °C are given in Figure 12. Only a single endotherm is observed over all the studied crystallization temperature ranges. Moreover, as expected for such NIFC crystals, their melting temperature increases against the crystallization temperature (Figure 13). A careful examination of this figure shows that the experimental data are distributed on two well-distinct curves corresponding to either (100) or (010) growth directions in the spherulites. Indeed, modifications of the spherulitic growth face

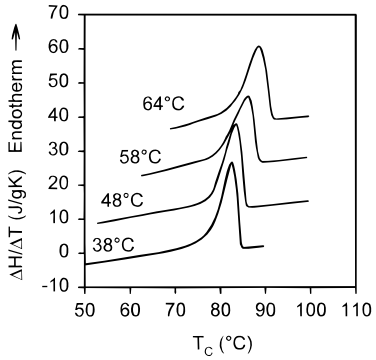

Figure 12. Melting curves of PEO6K−PNP samples crystallized from the melt at various temperatures (heating rate: 10 °C/min).

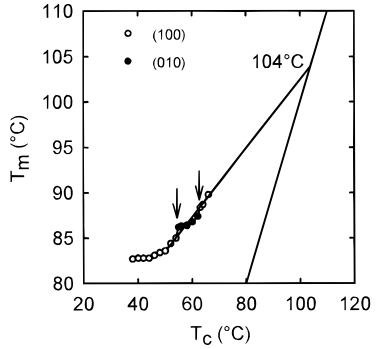

Figure 13. Melting temperature of PEO6K−PNP samples versus the crystallization temperature. The equilibrium melting temperature of (100) spherulites, T_m^0, is equal to 104 °C (heating rate: 10 °C/min). The transition temperatures between spherulitic growth faces are also indicated.

occur at 56 and 63 °C for PEO−PNP.[24] Lamellar crystals with different growth faces have a different dependence of their melting temperature versus their crystallization temperature. The equilibrium melting temperature (T_m^0) of PEO6K−PNP crystals with (100) growth faces is estimated to be 104 °C following the Hoffman−Weeks procedure.[30]

Time-Resolved Small Angle X-ray Scattering Measurements. SAXS intensity curves have been recorded during the heating of samples of PEO−RES and PEO−PNP molecular complexes from room temperature until their melting to investigate the change in their lamellar structure.

PEO6K−RES Molecular Complex. The SAXS intensity curves of a PEO6K−RES sample crystallized at 45 °C were recorded during the heating. The values of the first four long spacings are given against the temperature in Figure 14. The lamellar thickness keeps a constant value of 38.2 nm for temperatures lower than 75 °C. Afterwards, between 75 and 90 °C, the long spacing rapidly increases to reach the ultimate value of 41 nm. The second and third orders of the long spacing show the same behavior (Figure 14). As the first Bragg spacing corresponds to the lamellar thickness of EC crystals where the PEO chains are assumed to be perpendicular to the basal planes of the lamellae, any crystal rearrangement cannot be invoked to explain an increase of 3 nm of the long spacing of EC crystals. Such an increase of the lamellar thickness can thus be explained by considering the polydispersity of the PEO oligomers and a partial melting of the sample. Let us note that the values of the $\langle M_n^* \rangle$ number-average molecular weight calculated from the lamellar thicknesses of 38.2 and 41 nm are equal to 6882 and 7387,

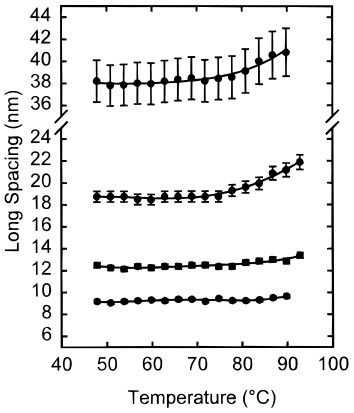

Figure 14. Values of the first four orders of the long spacing of PEO6K−RES lamellar crystals versus temperature.

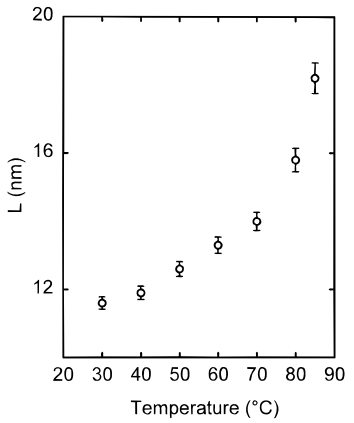

Figure 15. Long spacing of NIFC PEO6K−PNP lamellar crystals versus temperature.

respectively. These $\langle M_n^* \rangle$ values are quite understandable if one assumes a continuous melting of the thinnest EC lamellar crystals. The maximum of the chain length distribution at 75 °C is shifted to a higher value because the low molecular weight PEO chains are excluded from the computing of the most probable chain length at this temperature.

PEO6K−PNP Molecular Complex. The Lorentz-corrected SAXS intensity curves were recorded during the heating of a PEO6K−PNP sample crystallized at 60 °C. The observed long spacings increase with the temperature, starting from 11.4 to reach 18.2 nm just before complete melting (Figure 15). The annealing of the NIFC crystals starts at a very low temperature (40 °C), but the increase of the lamellar thickness becomes more important above 70 °C, where the thickening of the NIFC lamellar crystals of PEO6K−PNP easily occurs. It was very surprising to observe that these NIFC lamellar crystals are stable even close to the melting temperature and never transform into integral folded chain crystals. This behavior is quite different from the observations reported by Cheng et al.[11,12] for the crystallization of pure PEO oligomers from the melt: NIFC crystals, associated with the initial stages of crystallization, were assumed to be unstable and quickly transform into integral folded chain crystals following a thickening or thinning process.

Conclusions

SAXS and calorimetry investigations show that the PEO−RES molecular complex crystallizes from the melt with either extended chain or a small number of integral folded chains depending on the crystallization temper-

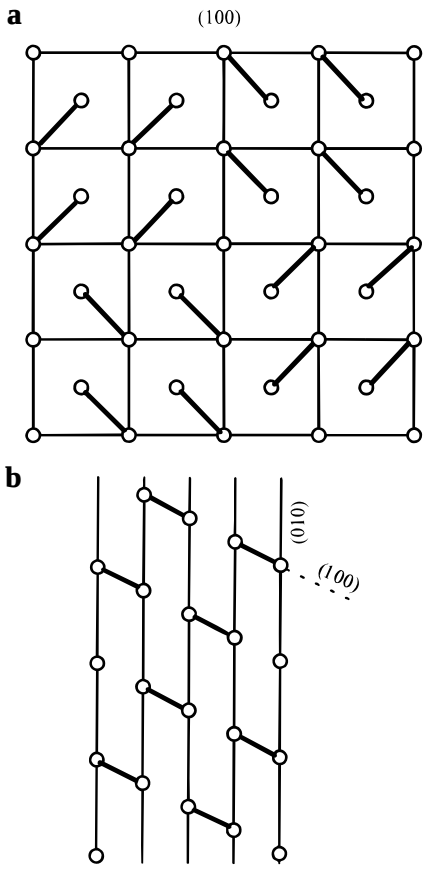

Figure 16. Schematic description of possible fold plane for PEO−RES (a) and PEO−PNP (b) molecular complexes.

ature and the molecular weight as already observed for pure PEO oligomers. However, the PEO−PNP complex surprisingly crystallizes as NIFC crystals over the entire range of crystallization temperatures. Moreover, as shown by the SAXS intensity curves recorded during the heating of PEO−PNP complexes, the observed lamellar thickness of these NIFC crystals continuously increases with temperature but never reaches extended chain conformation. These NIFC crystals thus never transform, even for long annealings at elevated temperatures, into integral folded chain crystals. These experimental results clearly show that the crystal structure and the mode of crystal growth play a major role in the formation of lamellar crystals of molecular complexes made of PEO and disubstituted benzenic molecules. Despite the similarity between both complexes made of the same macromolecule and similar substitued aromatic molecules, they crystallize from the melt with completely different morphologies (*x*IFC or NIFC). However, the possible fold planes deduced from the crystal structure may account for the observed difference in the lamellar thickness. Indeed, for the PEO−RES, the fold plane corresponds very likely to a (110) plane (Figure 16a), and for the PEO−PNP, the fold plane may be either (100) or (010), the latter corresponding to a very loose fold (Figure 16b). The rightness of these assumed fold planes will be confirmed by a study of single-crystal morphology now in progress.

Acknowledgment. This work was supported by the Belgian National Fund for Scientific Research (FNRS). Thanks are also due to the Science Programme of the European Union for access to the synchrotron radiation facilities at Lure (Centre Universitaire de Paris-Sud, Orsay, France).

References and Notes

(1) Arlie, J. P.; Spegt, P.; Skoulios, A. *Makromol. Chem.* **1966**, *99*, 160.
(2) Arlie, J. P.; Spegt, P.; Skoulios, A. *Makromol. Chem.* **1967**, *104*, 212.
(3) Spegt, P. *Makromol. Chem.* **1970**, *140*, 167.
(4) Kovacs, A. J.; Gonthier, A. *Kolloid. Z. Z. Polym.* **1972**, *250*, 530.
(5) Fenton, D. E.; Parker, J. M.; Wright, P. V. *Polymer* **1973**, *14*, 589.
(6) Hartley, A.; Leung, Y. K.; Booth, C.; Sheppard, I. W. *Polymer* **1988**, *29*, 579.
(7) Song, K.; Krimm, S. *Macromolecules* **1990**, *23*, 1946.
(8) Buckley, C. P.; Kovacs, A. J. *Prog. Colloid Polym. Sci.* **1975**, *58*, 44.
(9) Buckley, C. P.; Kovacs, A. J. *Colloid Polym. Sci.* **1976**, *254*, 695.
(10) Song, K.; Krimm, S. *Macromolecules* **1989**, *22*, 1504.
(11) Cheng, S. Z. D.; Zhang, A.; Chen, J. J. *J. Polym. Sci., Polym. Lett.* **1990**, *28*, 233.
(12) Cheng, S. Z. D.; Chen, J. J.; Wu, S. X.; Zhang, A.; Yandrasatis, M. A.; Zhuo, R.; Quirk, R. P.; Habenschuss, A.; Zschack, P. R. *NATO Series C* **1993**, *405*, 51.
(13) Kim, I.; Krimm, S. *Macromolecules* **1994**, *27*, 5232.
(14) Iwamoto, R.; Saito, Y.; Ishihara, H.; Tadokoro, H. *J. Polym. Sci., A2* **1968**, 1509.
(15) Yokoyama, M.; Ishihara, H.; Iwamoto, R.; Tadokoro, H. *Macromolecules* **1969**, *2*, 589.
(16) Tadokoro, H. *Macromol. Rev.* **1967**, *1*, 119.
(17) Chatani, Y.; Okoyama, X. *Polymer* **1987**, *28*, 1815.
(18) Point, J. J.; Coutelier, C. *J. Polym. Sci., Polym. Phys. Ed.* **1985**, *23*, 231.
(19) Myasnikova, R. M.; Titova, E. F.; Obolonkova, E. S. *Polymer* **1980**, *21*, 403.
(20) Delaite, E.; Point, J. J.; Damman, P.; Dosière, M. *Macromolecules* **1992**, *25*, 4768.
(21) Belfiore, L. A.; Veda, E. *Polymer* **1992**, *33*, 3833.
(22) Myasnikova, R. M. *Vysokomol. Soyed.* **1977**, *A19*, 564.
(23) Paternostre, L.; Damman, P.; Dosière, M., To be submitted.
(24) Damman, P.; Point, J. J. *Macromolecules* **1993**, *26*, 1722.
(25) Point, J. J.; Damman, P. *Macromolecules* **1992**, *25*, 1184.
(26) Villers, D.; Dosière, M.; Paternostre, L. *Polymer*, **1994**, *35*, 1586.
(27) Vonk, C. G.; Kortleve, G. *Kolloid. Z. Z. Polym.* **1967**, *220*, 9.
(28) Strobl, G. R.; Schneider, M. *J. Polym. Sci., Polym. Phys. Ed.* **1980**, *18*, 1343.
(29) Paternostre, L.; Damman, P.; Dosière, M. To be submitted.
(30) Hoffman, J. D.; Weeks, J. J. *J. Chem. Phys.* **1965**, *42*, 4301.

MA9506288